On The Effectiveness of The Proposed Illawarra Offshore Wind Farm

2024 HSC Science Extension Research Report
Smith's Hill High School

Student Number: 37115584

SUBMISSION 06/08/2024

Acknowledgements

Many thanks to George Takacs, University of Wollongong, for mentoring me as I wrote this paper. Your insight into meteorology, wind farms, and ability to problem solve was crucial in the creation of this paper.

Many thanks to Ms Parkinson, Smiths Hill High School, for helping me write the paper and providing me with guidance. And also for being an amazing science teacher :)

Abstract

Computational modelling was used to gain an understanding of the extent to which the proposed Illawarra offshore wind farm will overcome seasonal variability in solar production to provide New South Wales (NSW) and the Australian Capital Territory (ACT) with year-round renewable energy. Two Support Vector Machine (SVM) regression models were used to predict electricity demand and rooftop solar production based on population-weighted meteorological conditions. The amount of energy generated by the wind farm was predicted using the generation curve of a Vestas V164 turbine. Results from the simulation indicate that the wind farm will meet 3.5% of electricity demand in NSW and the ACT, with variance occurring at small time scales. Observed variance in wind production was not seasonal in nature, indicating an ability for the wind farm to meet demand during periods of low solar production.

Literature Review

The variable power output of renewable energy infrastructure remains a key concern when considering the integration of renewable energy sources into the grid. By the nature of their operation, the amount of power generated by renewable infrastructure is dependent upon the immediate, localised weather conditions at the generation site. Through the creation of a variety of forecasting models, Alrashidi et al. were able to determine the correlation between meteorological variables and electricity generated from a rooftop solar array (2023). The study trained a variety of computational models on time, weather and historical generation values to compare the prediction accuracy for future solar generation. The SVR model had the highest accuracy, achieving a root mean squared error (RMSE) of 14.52kW. A correlation coefficient of 0.95 was observed between solar irradiance and array output.

This weather dependence persits with wind generation infrastructure, as ascertained through an analysis of wind generation in the United States (Wan, 2012). The study determined that short term (minute-by-minute) variation in generation was stochastic in nature, with patterns emerging over larger time frames. Seasonal variation in single-turbine production aligned closely with local wind patterns, meaning that trends could not be established across separate wind farms. This minimises the applicability of findings from other wind farms to the Illawarra.

Variability of Demand

Changing weather conditions also influence energy demand, as consumer behaviour responds to immediate meteorological conditions. The effect of temperature on demand was studied by Le Comte et al., through an examination of the connection between heating and cooling days (HDD & CDD respectively) and energy demand in the United States (1981). The study scaled climate data according to population density, as more populated regions have greater electricity demand. This larger demand increases the influence of weather in these regions, which is replicated in the model through the scaling process.

De Cian et al. studied weather-induced demand variability by analysing a dataset of energy demand in 31 countries (2013). The study used mean temperature as the independent variable, and studied its effects on demand in three groups of countries (“hot”, “mild” and “cold”). An error correction regression model was used to determine how temperature affects demand in each country. It was observed that heat-waves had a greater impact on demand in “hot” countries, with cold-snaps having a greater impact on “cold” countries as seen in Figure 1.1

Figure 1.1

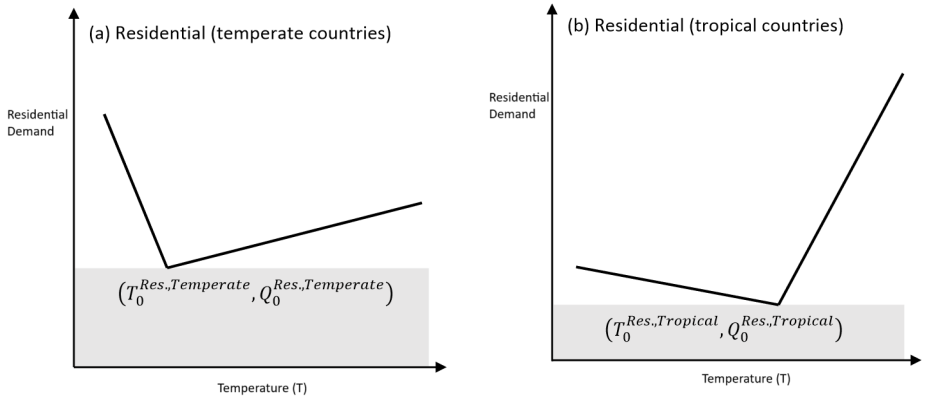

Two charts comparing how temperature affects residential electricity demand in temperate and tropical countries (Wing et al. 2016)

This methodology is limited through the classification of countries into 3 distinct groups. The study used hierarchical cluster analysis to determine which category each country fell within, however this technique only considers average temperature. As such, countries with highly variable temperatures may not be accurately categorised within the model. Additionally, the comparison of data across different countries introduces validity issues through the potential for non-standardised data collection methods across the 31 countries. This issue is present for energy consumption data and meteorological observations.

Role of Modelling

The variability of demand and supply necessitates the creation and application of forecasting techniques to ensure new renewable energy infrastructure addresses the needs of the community.

Prior works have established the suitability of Support Vector Machine (SVM) regression models to predict power demand. Through analysing power generation in Guangdong Province, China, Chen et al. evaluated the ability for various computational models to predict power demand (2023). The study compared SVM, linear regression and random forest models, with the SVM having the lowest root mean squared error (RMSE) of 0.089 when predicting capacity factor. The models used maximum and minimum temperatures, wind speed, precipitation and consumer price index to predict power demand over a year.

SVM models have also been shown to provide accurate forecasts of renewable energy generation (Huang et al. 2019)(Alrashidi et al. 2023). Ryu et al. studied the accuracy of different forecasting models for predicting the energy generation of a wind turbine in Yeonggwang-gun Province, South Korea (2022). The study trained a variety of machine learning models using generation data from a coastal turbine and weather data from a nearby weather station. The paper compared SVM, ARIMA, MLR and ARIMAX models, concluding that the SVM model had the lowest RMSE of 30.72KW.

As such, SVM models are an appropriate tool to predict power demand and solar production, having the ability to replicate real-world trends at a variety of time scales. This will allow an understanding of how the offshore wind farm compliments varying outputs from other renewable sources to meet demand. By comparing the variability of power generated from solar and wind infrastructure, an insight into the suitability of the wind farm can be gained.

Research Question

Does the proposed Illawarra Offshore Wind Farm have the ability to offset seasonal variance in power generation from other renewable energy sources?

Hypothesis

Through exhibiting generation variance at shorter time scales (day-by-day), the Illawarra wind farm will offset longer-term, seasonal variance in production from other renewable energy sources.

Methodology

The creation of weather-dependent energy models required the collection of a large amount of meteorological data. This data was sourced from the Bureau of Meteorology (BOM) climate maps archive, as this source included spatial variation in weather conditions (2024). The representation of spatial variance in the data was necessary to replicate the population normalisation method proposed by Le Comte et al. (1981). A custom web scraper was used to download the maps. Each cell in the map represents an area covering 0.05 degrees of latitude and longitude over a 24 hour period. Data for the meteorological variables shown in Figure 2.1 was collected for the period from 1/01/2019 to 31/03/2014.

Figure 2.1

Variable Name	Units	Mean	Standard Deviation
Temperature	°C	22.88	4.883
Solar Irradiance	MJ/m^2	16.478	6.675
Pressure	hPa	14.694	4.708
Rainfall	mm	3.353	8.329

Table showing the collected meteorological variables and basic descriptive statistics for the training period (01/01/2019-31/03/2024)

To perform the population normalisation, population density data from the Australian Bureau of Statistics was used (ABS, 2023). A Python script was developed to convert the GEOTIFF-encoded ABS data into a standardised GRID format. This process also involved the use of a custom processing pipeline to reduce the resolution of the map by combining cells into groups of nine. The sum of each group was then used as the value for the new, lower-resolution map (822x455 cells). This process is shown in Figure 2.2, and was done to ensure the cell-size of the density data closely matched the meteorological data.

Figure 2.2

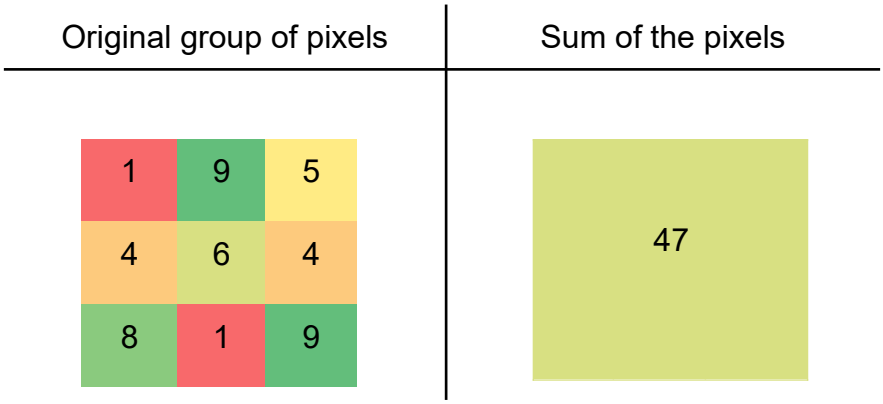

Diagram showing the influence of the cell summing process on a 3x3 array of pixels. The sum of all 9 pixels is the value of the new pixel.

A data-processing pipeline was then used to determine the population-weighted weather value for each day. The cell value was calculated by multiplying the climate variable by the population at the same location. The sum of these values was then divided by the total population of NSW and the ACT to determine the daily population-weighted mean, as shown in Figure 2.3. This process was applied to 9,567 cells for each day and meteorological variable.

Figure 2.3

$$\text{Cell Value} = \text{Climate Value} \times \text{Population in Cell}$$

$$\text{Population Weighted Mean} = \sum \frac{\text{Cell Value}}{\text{Population}}$$

Formula for the population weighted mean for a given day and meteorological variable

ERA5 reanalysis data was used to determine the wind velocity for a point within the proposed area for the wind farm (34.47°S, 151.29°E) (C3S, 2023). NASA's Panoply visualisation tool was used to convert the ERA5 data into a list of values. (NASA, 2024). The studied location is 35km offshore, as shown in Figure 2.4.

Figure 2.4

Map showing location of the studied wind values (34.47°S, 151.29°E)
(Google, 2024)

Another web-scraper was then used to download energy data for the NSW region from OpenNEM (McConnel, 2024). The energy data covered the same time period as the weather data, with a data processing pipeline being used to convert the json-encoded NEM data into a csv file. The pipeline also normalised daily solar production to account for increasing solar capacity across Australia. This was achieved by dividing the daily solar production value by the capacity of solar infrastructure across Australia (Australian Photovoltaic Institute, 2023). Figure 2.5 shows the reduction in year-on-year variance associated with this normalisation process.

Figure 2.5

Raw Values	Normalised Values

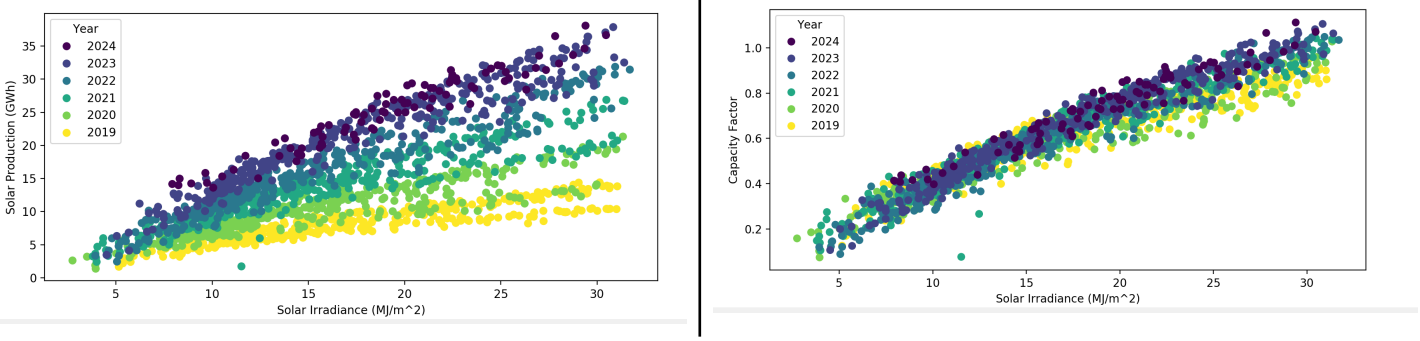

Two scatter plots comparing the spread of data before and after the normalisation process

The daily population-weighted weather variables and NEM data was used to train two Support Vector Machine (SVM) models. The demand model used a Radial Basis Function (RBF) kernel, with the solar production model using a linear kernel. Both models received a 5-dimensional dataset as input, containing the 4 climate variables and the day of the year. 1515 data points were used to train the SVM models, with the remaining 400 data points being used to determine the RMSE of each model. The training parameters are shown in Figure 2.6.

Figure 2.6

Model Type	Kernel Type	Gamma Value	C-Value
Demand	Radial Basis Function	0.1	1
Solar	Linear	0.2	3

Training Parameters for the two SVM models

Based on publicly available information about the Illawarra wind-farm, the study assumed the wind farm would use 100 Vestas V164 wind turbines (South Pacific Offshore Wind Project, 2022). Single-turbine generation values were determined by inputting collected wind speeds into the power generation curve for the V164, as shown in Figure 2.7. This process was replicated for each of the 100 turbines that make up the wind farm.

Figure 2.7

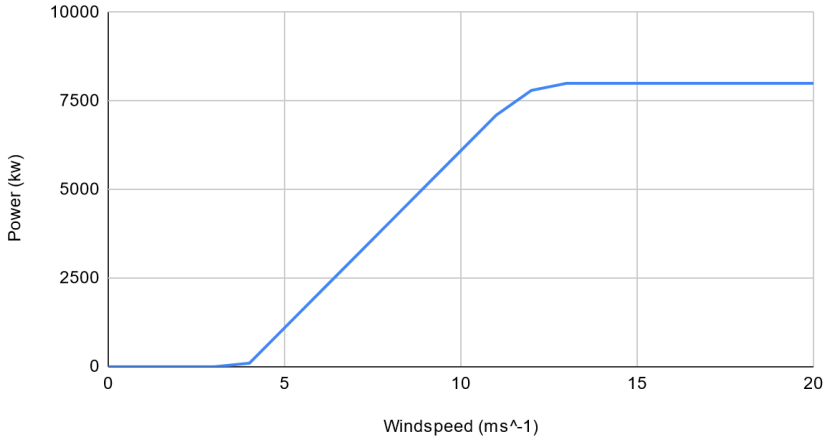

Power generation curve for a Vestas V164 Turbine

The two SVM models, wind turbine model, and climate data were then combined into a single simulation. Real-world meteorological conditions from 01/01/2016 to 31/04/2024 were then input into the model to assess the effectiveness of the wind farm. The meteorological variables were downloaded and processed using the same method as the training data. The effectiveness of solar and wind infrastructure was determined through three metrics that describe the amount of demand being met by each resource. These metrics are outlined in Figure 2.8, with an ANOVA test being used to compare the mean solarPortion and windPortion for the 4 seasons.

Figure 2.8

Metric Name	Description	Formula
solarPortion	Portion of demand met by solar infrastructure	$\text{SP} = \frac{\text{Energy Produced by Solar}}{\text{Total Energy Demand}}$
windPortion	Portion of demand met by the Illawarra wind farm	$\text{WP} = \frac{\text{Energy Produced by Wind Farm}}{\text{Total Energy Demand}}$
renewablePortion	Portion of demand met by both solar & wind farm	$\text{RP} = \frac{\text{Energy Produced by Wind Farm} + \text{Energy Produced by Solar}}{\text{Total Energy Demand}}$

Table showing the three metrics used to assess the wind farm

Results

Figure 3.1

Day of the Year vs total Demand

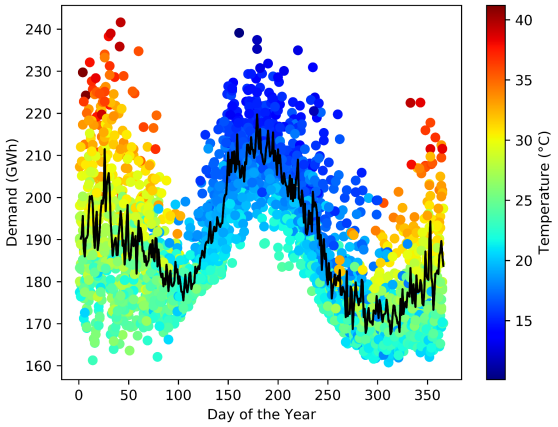

Mean Daily Demand = 187.99 GWh

Figure 3.2

Temperature vs Predicted Demand

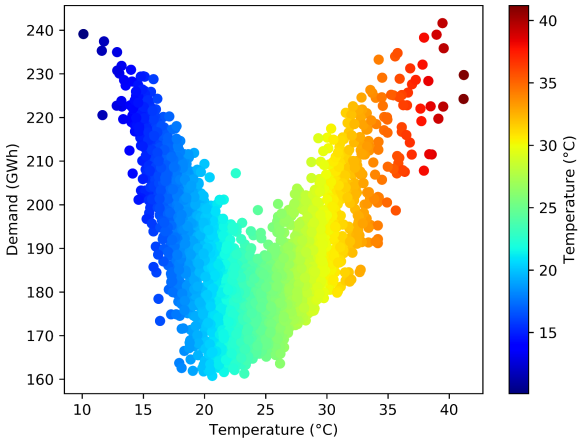

Mean Temperature = 23.02°C

The demand and solar models achieved a RMSE of 0.540GWh and 0.228GWh respectively for the training period. These models were then applied to meteorological conditions from 01/01/2016 to 31/03/2024 (n=3011). By plotting demand against day of the year, Figure 3.1 demonstrates its seasonal fluctuation, with greater demand in summer and winter and lower demand in autumn and spring. The temperature dependent nature of this relationship is shown in Figure 3.2, with extreme temperatures causing large increases in demand.

Figure 3.3

Daily Solar Production Vs Day of the Year

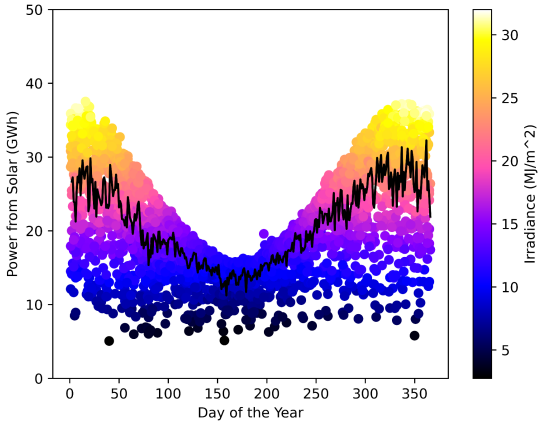

Mean Daily Energy Production (Solar) = 20.81 GWh

Figure 3.4

Daily Wind Production vs Day of the year

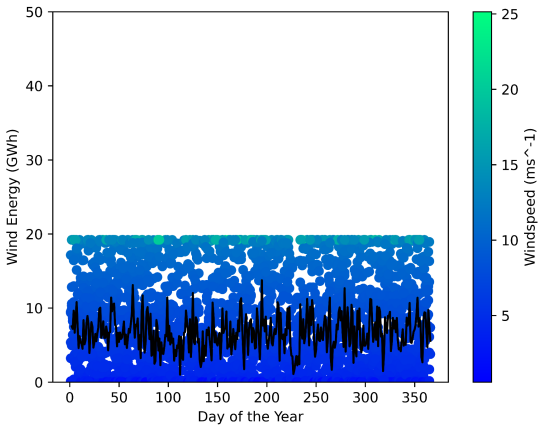

Mean Daily Energy Production (Wind) = 6.61 GWh

Figure 3.3 shows predicted solar energy generation by day of the year. It is notable that the decrease in winter-time solar production occurs at the same time as the increase in demand during this period seen in Figure 3.1. Figure 3.4 shows wind farm energy production by day of the year. A significant amount of short-term variation is observed, however no seasonal trends are visible. As each wind turbine cannot produce more than 8 MW of energy, the wind farm as a whole is limited to generating 19.2 GWh of electricity each day, resulting in a defined upper limit.

Figure 3.5

Day of the Year vs Solar Portion

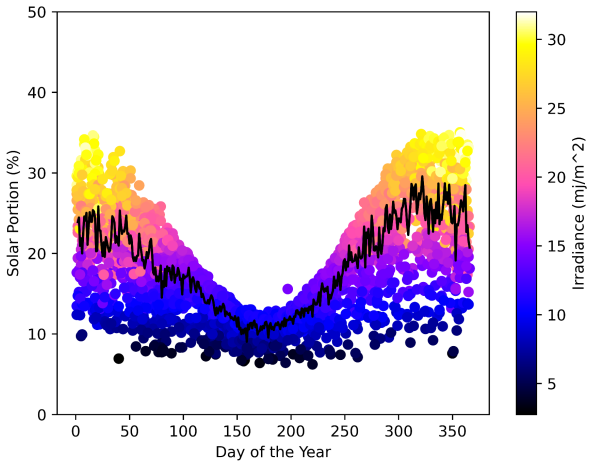

Mean Solar Portion = 18.6%

Figure 3.6

Day of the Year vs Renewable Portion

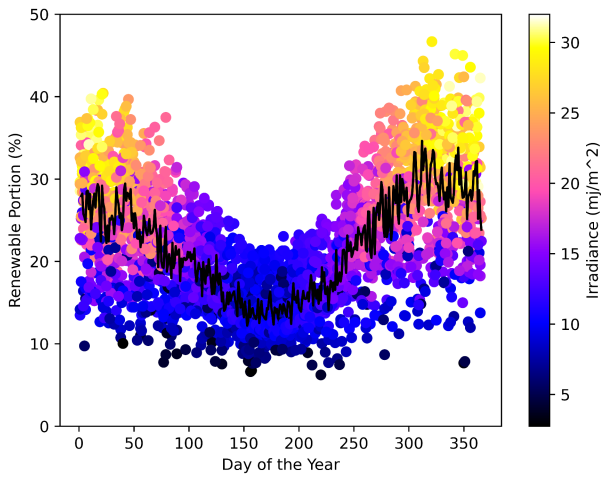

Mean Renewable Portion = 22.1%

By considering the portion of demand met by solar infrastructure, Figure 3.5 shows how increasing demand and decreasing supply in the winter substantially lowers the portion of demand met by solar infrastructure. Figure 3.6 shows the portion of demand met by renewable sources over time. This still contains a dip in the winter, however the inclusion of the wind farm results in an increase in winter-time renewable energy portions. In this regard, the insensitivity of the wind-farm to seasonal variation increases the portion of demand met from renewable sources by an average of 3.5% over the studied period.

Figure 3.7

Portion of demand met by renewable resource for each season (%)

Source	Summer	Autumn	Winter	Spring	Whole Year
Solar	23.2	15.7	12.4	20.9	18.6
Wind	3.7	3.2	3.2	3.7	3.5
Solar + Wind	26.9	18.9	15.6	24.5	22.1

Figure 3.8

ANOVA results for seasonal variance in the portion of demand met by the two generation methods

α Value: 0.01

H0: The season will have no impact on the portion of demand met by each energy source

H1: The season will have an impact on the portion of demand met by each energy source

Source	P-Value	Accept/Reject the Null Hypothesis
Solar	4.14505911E-113	Reject
Wind	0.00016468	Reject

Figure 3.7 shows the portion of demand met by wind and solar infrastructure across the 4 seasons. An ANOVA test was conducted to assess this difference, with the results shown in Figure 3.8. The test was able to reject the null hypothesis for both generation methods, indicating a statistically significant variation in the portion of demand met by both solar and wind infrastructure.

Figure 3.9

Portion of renewable energy (%) generated by the Illawarra offshore wind farm by season

Summer	Autumn	Winter	Spring	Whole Year
13.9	20.3	22.1	15.1	15.8

The importance of wind infrastructure to the renewable grid is shown in Figure 3.9, with the model predicting that the Illawarra offshore wind farm could supply 22.1% of all renewable energy in winter time. The change in these values occurs as a result of consistent output from the wind farm at seasonal time scales compared to the highly variable solar output. This demonstrates wind farm's ability to offset seasonal variance in solar energy production. Across the studied period, the wind farm achieved an average capacity factor of 0.344 (Appendix A).

Discussion

The results indicate a high likelihood that the proposed Illawarra offshore wind farm will not experience seasonal variance in energy production. Computational modelling indicates a statistically significant seasonal variation in the portion of demand met by both solar and wind infrastructure. However, the magnitude of this seasonal variance was observed to be less for the proposed wind farm. This is shown in Figure 3.9, as the portion of renewable energy generated by wind infrastructure increases during winter.

Modelling indicates that the wind farm would meet an average of 3.5% of electricity demand in NSW and the ACT. This would save 2.177 megatonnes of CO_2 emissions annually compared to a black coal power plant producing the same amount of electricity (Jotzo and Mazouz, 2015) (Appendix B & C). Demonstrating the ability for the windfarm to cause a reduction in greenhouse gas emissions.

Simulated wind farm outputs produced a capacity factor of 0.344 (Appendix A). This value closely matches industry norms, with the United States having a grid-wide capacity factor of 0.35 for wind farms (Wiser and Bolinger, 2022). The modelling also reaffirmed the predominantly stochastic nature of short-term fluctuations in wind energy production as described by Wan (2012). A large degree of variance was observed at short (day-by-day) time scales, however variance was not observed at larger time scales. This indicates a lack of seasonal trends in wind speed within the Illawarra, showing the value of the region for offshore wind production. The observed reduction in the portion of demand met by wind infrastructure during the winter occurred as a result of increased demand during this period, rather than decreased supply from the wind-farm. This is shown in Figures 3.4 and 3.1 respectively. The ANOVA test was repeated with raw generation values, and did not produce a statistically significant seasonal variance in wind energy generation (Appendix D).

The demand model was unable to replicate the levels of accuracy exhibited by similar methods. Chen et al.’s SVM model achieved an RMSE value of 0.089 (as a capacity factor) whilst predicting electricity demand in Guangdong province, China (2023). This difference in accuracy arose as a result of the differing inputs into the models. Chen et al.'s method used demand for the previous day as a data point to train the model. This method is only suitable for modelling the next day, as it requires knowledge of current-day grid conditions. Hence, it was not feasible for this investigation, which required long term

modelling capabilities. This reduced the accuracy of the developed model by limiting the amount of input data.

Despite the inaccuracies, the demand model replicated the temperature dependency of electricity demand. However, the model did not replicate the proposed influence of long-term climatic patterns on the temperature-demand relationship (De Cian et al., 2013). Simulated demand increased similarly irrespective of whether the temperature was above or below the mean. This could be explained by the moderate temperatures in NSW, having a mean temperature of 23.019°C during the studied period. The proposed relationship might have occurred if a region with a more extreme mean temperature was modelled.

The solar production model replicated the relationship between irradiance and solar energy production. An R^2 value of 0.994 was observed between simulated solar production and irradiance, supporting Alrashidi et al.'s results (2023). This dependence causes decreased solar production in winter, as shorter days and lower irradiance limit generation capabilities. The solar generation model was limited through its inability to predict the output of industrial solar generation plants. As these plants are generally located outside of populated areas, the weighting of meteorological variables to bias populated areas worked against establishing a correlation between industrial solar production and the weighted meteorological variables (Renew Economy, 2024). Future research could conduct a reanalysis of the meteorological data to bias it towards the locations of industrial solar farms, allowing more accurate prediction of industrial solar production.

The study was limited through its 24 hour temporal resolution. As the available meteorological and grid data was reported at 24 hour intervals, the study was unable to consider grid operation at hourly time scales. Future investigations could examine the ability for the offshore wind farm to meet demand during the early morning or evening, when solar irradiance is significantly lower. Future studies could also apply the developed simulation to determine the optimal generation curve for wind turbines for the proposed area.

Conclusion

Computational simulations indicate that the Illawarra offshore wind farm will meet approximately 3.5% of NSW's and the ACT's electricity demand. Seasonal variance in solar production was observed, as generation peaked in summer and declined in winter. The simulated wind farm exhibited variance at daily time scales, however did not exhibit variance at seasonal scales. Both solar and wind infrastructure exhibited a statistically significant seasonal variance in the portion of demand supplied, However, only solar infrastructure exhibited this variance with raw generation values. In this regard, the wind farm was found to have the ability to offset seasonal variance in solar production through exhibiting variance at shorter time scales.

The modelling predicted that the installation of the wind farm will save 2.177 megatonnes of CO_2 emissions annually compared to equivalent power generation from coal-fired power plants. The developed models replicated real-world trends in both demand and solar production, including the temperature dependence of demand and the relationship between solar irradiance and solar cell production.

Word Count

Section	Word Count
Abstract	138
Literature Review	751
Research Question & Hypothesis	47
Methodology	709
Results	449
Discussion	738
Conclusion	165
Total	**2997**

References

Sources

Alrashidi, Musaed, and Saifur Rahman. 2023. “Short-Term Photovoltaic Power Production Forecasting Based on Novel Hybrid Data-Driven Models.” *Journal of Big Data* 10 (1): NA-NA. https://doi.org/10.1186/s40537-023-00706-7.

Chen, Gang, Qingchang Hu, Jin Wang, Xu Wang, and Yuyu Zhu. 2023. “Machine-Learning-Based Electric Power Forecasting.” *Sustainability* 15 (14): 11299. https://doi.org/10.3390/su151411299.

De Cian, Enrica, Elisa Lanzi, and Roberto Roson. 2013. “Seasonal Temperature Variations and Energy Demand.” *Climatic Change* 116 (3): 805–25. https://doi.org/10.1007/s10584-012-0514-5.

Huang, Jianqiang, Ye Liang, Haodong Bian, and Xiaoying Wang. 2019. “Using Cluster Analysis and Least Square Support Vector Machine to Predicting Power Demand for the Next-Day.” *IEEE Access* 7:82681–92. https://doi.org/10.1109/ACCESS.2019.2922777.

Jotzo, Frank, and Salim Mazouz. 2015. “Brown Coal Exit: A Market Mechanism for Regulated Closure of Highly Emissions Intensive Power Stations.” *Economic Analysis and Policy* 48 (December):71–81. https://doi.org/10.1016/j.eap.2015.11.003.

Le Comte, Douglas M., and Henry E. Warren. 1981. “Modeling the Impact of Summer Temperatures on National Electricity Consumption.” *Journal of Applied Meteorology (1962-1982)* 20 (12): 1415–19. https://www.jstor.org/stable/26180364.

Renew Economy. 2024. “Large Scale Solar Farm Map of Australia.” https://reneweconomy.com.au/large-scale-solar-farm-map-of-australia/.

Ryu, Ju-Yeol, Bora Lee, Sungho Park, Seonghyeon Hwang, Hyemin Park, Changhyeong Lee, and Dohyeon Kwon. 2022. “Evaluation of Weather Information for Short-Term Wind Power Forecasting with Various Types of Models.” *Energies* 15 (24): 9403. https://doi.org/10.3390/en15249403.

South Pacific Offshore Wind Project. 2022. “Informational Poster.” https://static1.squarespace.com/static/61b6cf61e74b6554548d635d/t/64801dcedac576260cb6a96f/1686117857004/Informational%2BPosters.pdf.

Wan, Yih. 2012. “Long-Term Wind Power Variability.” NREL/TP-5500-53637, 1033036. National Renewable Energy Laboratory. https://doi.org/10.2172/1033036.

Wiser, Ryan, and Mark Bolinger. 2022. “Land-Based Wind Market Report: 2022 Edition: Executive Summary.” *US Department of Energy*. https://www.energy.gov/sites/default/files/2022-08/land_based_wind_market_report_2022_executive_summary.pdf.

Software

Hunter, John D. 2007. “Matplotlib: A 2D Graphics Environment.” *Computing in Science & Engineering* 9 (3): 90–95. https://doi.org/10.1109/MCSE.2007.55.

NASA Goddard Institute for Space Studies. 2024. “Panoply netCDF, HDF and GRIB Data Viewer.” Java. NASA. https://www.giss.nasa.gov/tools/panoply/.

Virtanen, Pauli, Ralf Gommers, Travis E. Oliphant, Matt Haberland, Tyler Reddy, David Cournapeau, Evgeni Burovski, et al. 2020. “SciPy 1.0: Fundamental Algorithms for Scientific Computing in Python.” *Nature Methods* 17:261–72. https://doi.org/10.1038/s41592-019-0686-2.

Datasets

Australian Bureau of Statistics. 2023. “Regional Population (2022-23).” Map. https://www.abs.gov.au/statistics/people/population/regional-population/latest-release#data-downloads.

Australian PV Institute. 2024. “Australian PV Market since April 2001.” https://pv-map.apvi.org.au/analyses.

Bauer, Lucas, and Silvio Matysik. n.d. “Compare Power Curves of Wind Turbines.” https://en.wind-turbine-models.com/powercurves.

Bureau of Meteorology. 2024. “Maps of Recent and Past Conditions.” Map. http://www.bom.gov.au/climate/maps/.

C3S. 2018. “ERA5 Hourly Data on Single Levels from 1940 to Present.” Copernicus Climate Change Service (C3S) Climate Data Store (CDS). https://doi.org/10.24381/CDS.ADBB2D47.

McConnell, Dylan, Simon Holmes à Court, Steven Tan, and Nik Cubrilovic. 2024. “OpenNEM.” https://opennem.org.au/energy/nem.

Figures

Cover Image

Furlong, Christopher, dir. 2008. *Burbo Bank Wind Farm Now Fully Operational*. Getty Images. https://www.gettyimages.com.au/detail/news-photo/turbines-of-the-new-burbo-bank-off-shore-wind-farm-stand-in-news-photo/81060825?adppopup=true.

Figure 1.1

Wing, Ian Sue, and Enrica De Cian. 2016. “Global Energy Demand in a Warming Climate.” Fondazione Eni Enrico Mattei (FEEM). https://www.jstor.org/stable/resrep15086.

Figure 2.4

Google. 2024. “Illawarra.” Google. https://www.google.com/maps/place/34%C2%B030'00.0%22S+151%C2%B020'24.0%22E/@-34.4135672,151.0686418,11.17z/data=!4m4!3m3!8m2!3d-34.5!4d151.34?entry=ttu.

Figure 2.6

Data is from Bauer et al., 2024

Appendix

Appendix A - Capacity Factor Calculations

$$\text{Annual Power Generated by Wind Farm} = 2,418,746 \text{ MWh}$$

$$\begin{aligned} \text{Capacity of a Single Turbine} &= 8\text{MW} \\ \text{Number of Turbines} &= 100 \\ \text{Number of Hours in a year} &= 365 \times 24 \end{aligned}$$

$$\begin{aligned} \therefore \text{Capacity Factor} &= \frac{\text{Energy Produced}}{\text{Max Possible energy Production}} \\ &= \frac{2,418,746}{8 \times 100 \times 365 \times 24} \\ &= 0.34515 \end{aligned}$$

Appendix B - Production Values

Figure 4.1

Infrastructure	Annually (GWh)	Total (Gwh) (3011 days)
Solar	12,629.724	104,187
Wind	2,418.746	19,953

Appendix C - Carbon Offset Calculations

Assuming generating 1MWh of electricity from a coal fired power plant produces 0.9 tonnes of CO2 emissions (Jotzo and Mazouz 2015)

$$\text{Total Power Generated by Wind Farm} = 19953 \text{ GWh}$$

$$\begin{aligned} \text{Yearly Average} &= \frac{19953}{3011 \div 365} \\ &= 2,418.746 \text{ GWh} \\ &= 2,418,746 \text{ MWh} \end{aligned}$$

$$\begin{aligned} \therefore \text{Annual Carbon Savings} &= 2418746 \times 0.9 \\ &= 2176871.637 \text{ Tonnes} \\ &= 2.1768 \text{ Mega Tonnes} \end{aligned}$$

Appendix D - ANOVA Test for Generation Values

Figure 4.2

Amount of energy generated by season and infrastructure type (GWh)

Source	Summer	Autumn	Winter	Spring	Total
Solar	25.9	17.6	15.4	24.4	83.3
Wind	7.0	6.1	6.6	6.9	26.6
Solar + Wind	32.9	23.7	22	31.3	109.9

Figure 3.8

ANOVA results for seasonal variance in the amount of energy generated by the two generation methods

α Value: 0.01

H0: There will be no difference in energy generated between the seasons

H1: There will be a difference in energy generated between the seasons

Source	P-Value	Accept/Reject the Null Hypothesis
Solar	1.22098866E-110	Reject
Wind	0.0320164	Accept

Code

The code is available on Github at https://github.com/gabriel-hanich/Compute-Power. It was written using Python, and only requires a couple of modules which can be downloaded using pip. Most of the raw data is in the Github, within the main/main/data/processed/sim folder.

Portfolio

The Portfolio document that details the creation of this report is available at https://docs.google.com/document/d/1Co7uDB_fqZUNIwXAXEXgNMjGEZBZbY-Wiu1MLQ1i2EQ/edit?usp=sharing